OPTIMAL DECISION FUSION IN THROUGH-THE-WALL RADAR IMAGING

Christian Debes[1], *Moeness G. Amin*[2] *and Abdelhak M. Zoubir*[1]

[1]Signal Processing Group
Technische Universität Darmstadt
Darmstadt, Germany

[2]Center for Advanced Communications
Villanova University
Villanova, PA, USA

ABSTRACT

We consider the problem of target detection behind walls based on optimum decision fusion using Neyman-Pearson tests. A framework, demonstrating the use of multiple sensor platforms and distributed detection for the emerging application area of Through-the-Wall Radar Imaging is presented. We derive the optimum decision rule at the fusion center for three dissimilar sensors and compare the corresponding target detection results to that achieved when using a centralized decision approach. Real data generated using a two dimensional scanning system is used for the performance comparison.

Index Terms— Through-the-wall, radar imaging, distributed detection, decision fusion

1. INTRODUCTION

Through-the-Wall (TTW) Radar Imaging is an emerging technology involving cross-disciplinary research in electromagnetic propagation, antenna design, beamforming [1], detection [2, 3] and image processing [4]. Applications arise in numerous civilian, law enforcement and military sectors [5], making it an attractive tool in e.g. search and rescue operations or police and firefighter missions.

It has been shown [1, 2] that the use of more than one radar system improves the radar image quality and subsequently the probability of detection. When a set of radar images, representing the same physical content, is acquired, the question arises on how to fuse this set of images to a single common reference image. In [1] a simple pixelwise multiplication scheme was adopted, whereas in [2] the application of likelihood ratio tests [6] was explored. The approach considered herein is based on distributed detection [7, 8]. A set of detectors is used to compile individual decisions. The decisions from all systems are then forwarded to a fusion center which compiles the overall decision. Compared to centralized systems, distributed systems provide higher system reliability and reduced computational complexity.

In this paper, we introduce the framework of distributed detection and optimal decision fusion for use in Through-the-Wall Radar Imaging. We hereby restrict ourselves to distributed Neyman-Pearson tests. In Section 2 the concept of centralized fusion using Neyman-Pearson tests is shortly reviewed in the context of TTW radar imaging. Section 3 then introduces the distributed Neyman-Pearson test and the optimal decision rule at the fusion center. Experimental results, making use of the introduced centralized and decentralized detector, are shown in Section 4

The work by Moeness Amin is supported by ONR, grant no N00014-07-C-0413

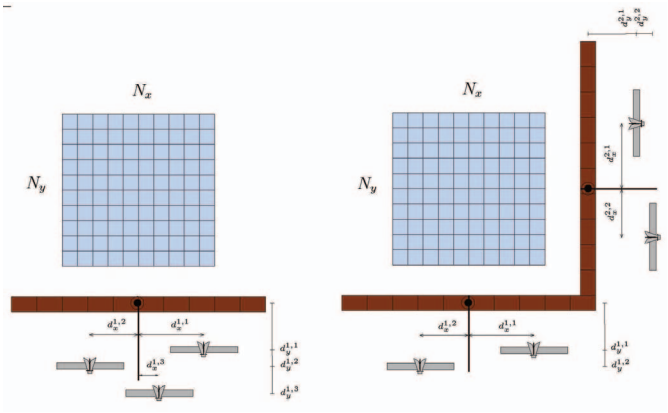

Fig. 1. Imaging through walls from multiple vantage points

2. CENTRALIZED FUSION

Let $B(i,j)$ with $0 \leq i < I$ and $0 \leq j < J$ denote a binary image, representing the true target locations within a B-Scan (crossrange vs. downrange 3D cut) of the hidden scene of interest, i.e.

$$B(i,j) = \begin{cases} 1 & \text{if a target is present at}(i,j) \\ 0 & \text{if no target is present at}(i,j) \end{cases} \quad (1)$$

Further, let $\{Y_k(i,j)\}_{k=1}^{K}$ denote the set of acquired TTW radar images, obtained from K vantage points. For this purpose, a set of TTW radars may be placed, illuminating different front or exterior walls, as depicted in Figure 1. The aim is to decide for $B(i,j)$ from $\{Y_k(i,j)\}_{k=1}^{K}$ in a statistical meaningful way.

In Figure 2, a centralized fusion scheme for use in TTW radar

978-1-4244-2710-9/09/$25.00 © 2009 IEEE

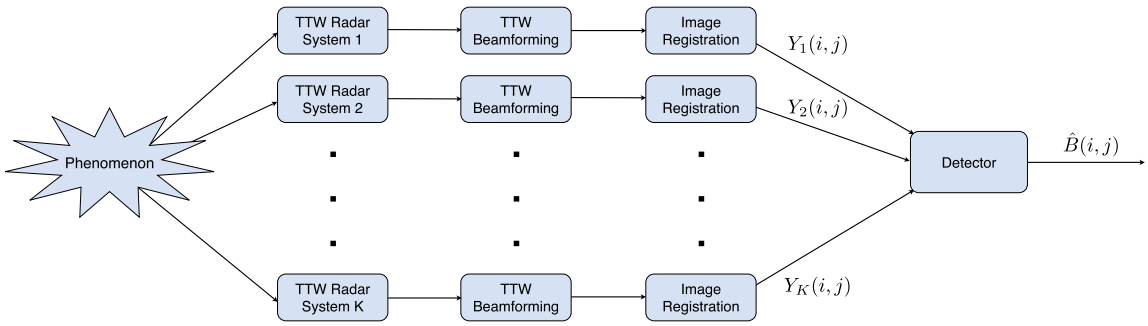

Fig. 2. Centralized Detection Framework

imaging is depicted along the same lines discussed in [2]. A set of K TTW radar systems is used to illuminate the scene of interest. A wideband beamformer [1] may be used to perform the imaging operation. As the radar images are obtained from different vantage points an image registration step is needed to align all images on a common grid. The resulting set of images $\{Y_k(i,j)\}_{k=1}^{K}$, $i = 1, ..., I$, $j = 1, ..., J$ is then passed to a detector which makes the final decision $B(i,j)$, $i = 1, ..., I$, $j = 1, ..., J$. This can be achieved using likelihood ratio tests (LRT) as in [2], assuming the data over k to be independent and identically distributed (i.i.d)

$$\text{LR}(i,j) = \prod_{k=1}^{K} \frac{p(Y_k(i,j)|H_1)}{p(Y_k(i,j)|H_0)} \underset{H_0}{\overset{H_1}{\gtrless}} \gamma \tag{2}$$

where H_0 and H_1 are the null and alternative hypotheses and γ is the likelihood ratio threshold which can be found by e.g. using the Neyman-Pearson lemma [6] with the preset level of test

$$\alpha = \int_{\gamma}^{\infty} p(L|H_0)dL \tag{3}$$

where $p(L|H_0)$ is the distribution of the likelihood ratio under the null hypothesis, H_0.

3. DECENTRALIZED FUSION

Figure 3 demonstrates the concept of decentralized fusion in TTW radar imaging. Here, the system 'intelligence' is distributed, meaning that each acquired image $Y_k(i,j)$, $i = 1, ..., I$, $j = 1, ..., J$ is followed by a local detector which passes its decision $B_k(i,j)$, $i = 1, ..., I$, $j = 1, ..., J$ for $k = 1, ..., K$ to a fusion center which then generates the global decision $B(i,j)$, $i = 1, ..., I$, $j = 1, ..., J$.
The advantages of the decentralized fusion scheme are

- Higher system reliability. A single detector which fails will not cause the whole system to fail
- The individual systems only pass binary information to the center which saves transmission capacity
- The fusion center can be very efficiently designed using simple boolean functions which saves computation

We follow the idea from [9], where the optimal decision scheme at the fusion center using the Neyman-Pearson test has been derived.
Given a set of binary decisions for one single pixel at location (i,j), $B_1(i,j), B_2(i,j), ..., B_K(i,j)$, which in the following will be denoted as $B_1, B_2, ..., B_K$, the Neyman-Pearson test at the fusion center given output B takes the form

$$\Lambda(B) = \frac{p(B1, B2, ..., B_K|H_1)}{p(B1, B2, ..., B_K|H_0)} \underset{H_0}{\overset{H_1}{\gtrless}} t \tag{4}$$

which reduces to

$$\Lambda(B) = \prod_{k=1}^{K} \Lambda(B_k) = \prod_{k=1}^{K} \frac{p(B_k|H_1)}{p(B_k|H_0)} \underset{H_0}{\overset{H_1}{\gtrless}} t \tag{5}$$

when assuming independence over k. The variable t is the likelihood ratio threshold at the fusion center used to tune the preset global false-alarm rate, α. Given α, t can be found via

$$\alpha = \sum_{\Lambda(B)>t} p(\Lambda(B)|H_0) = \sum_{\Lambda(B)>t} \prod_{k=1}^{K} p(\Lambda(B_k)|H_0) \tag{6}$$

The likelihood ratio $\Lambda(B_k)$ can take values

$$\Lambda(B_k) = \begin{cases} \frac{P_{D,k}}{\alpha_k} & \text{for } B_k = 1 \\ \frac{1-P_{D,k}}{1-\alpha_k} & \text{for } B_k = 0 \end{cases} \tag{7}$$

where $P_{D,k}$ and α_k denote the probability of detection and the probability of false-alarm for the image k, respectively. Further

$$p(\Lambda(B_k)|H_0) = \begin{cases} \alpha_k & \text{for } B_k = 1 \\ 1-\alpha_k & \text{for } B_k = 0 \end{cases} \tag{8}$$

3.1. Three dissimilar detectors

The optimal decision scheme for three dissimilar sensors will be shown in the following. Experimental results using three

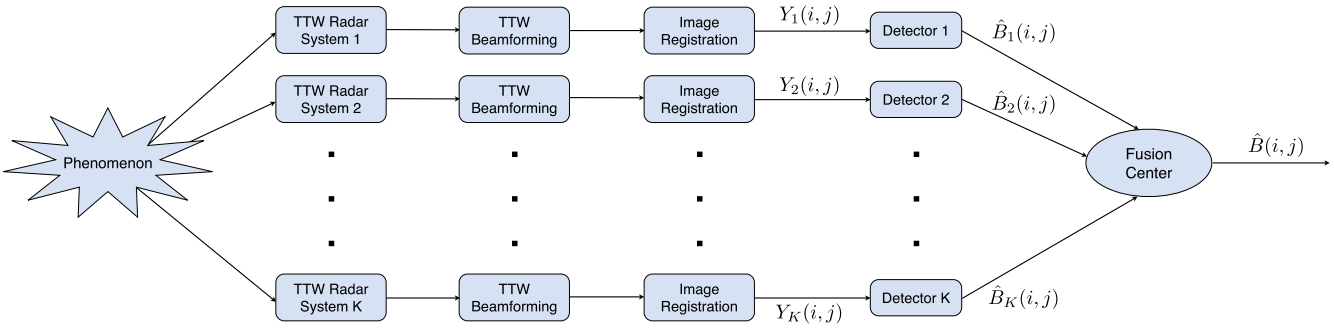

Fig. 3. Distributed/Decentralized Detection Framework

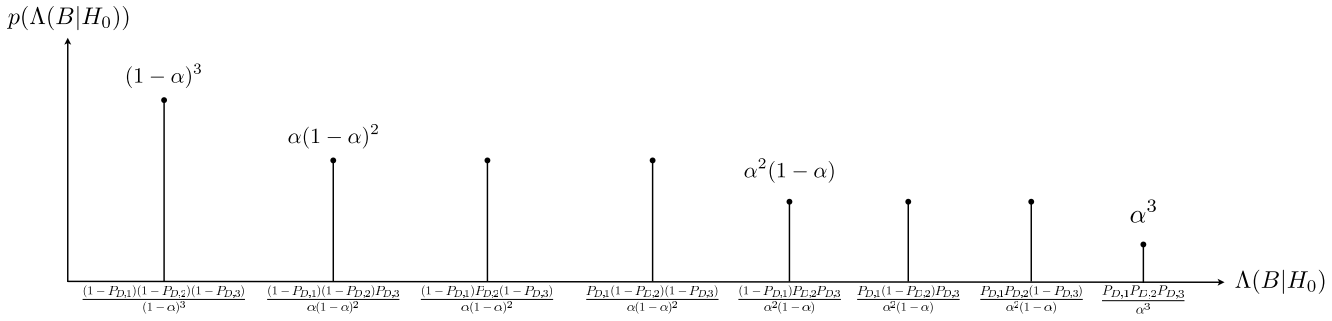

Fig. 4. $p(\Lambda(B)|H_0)$ for three dissimilar sensors

dissimilar sensors will be provided in the next section.

Let $\alpha_k = \alpha_0 \ \forall \ k$, i.e. all local detectors operate at the same false-alarm rate. Further, let $P_{D,1}, P_{D,2}$ and $P_{D,3}$ denote the corresponding probabilities of detection where without loss of generality we assume $P_{D,1} > P_{D,2} > P_{D,3}$. Note that the image statistics vary from vantage point to vantage point which causes different probabilities of detection given the same false-alarm rate at all detectors. The corresponding distribution of the likelihood ratio for three dissimilar sensors can be obtained by evaluating Equations (7) and (8). The resulting distribution is depicted in Figure 4. It can be shown that in order to achieve a global false-alarm rate identical to the local false-alarm rates, i.e. $\alpha = \alpha_0$, a randomized Neyman-Pearson test with threshold

$$t = \frac{P_{D,1}(1-P_{D,2})(1-P_{D,3})}{\alpha(1-\alpha)^2} \tag{9}$$

and randomization constant

$$\omega = \frac{2\alpha - 1}{\alpha - 1} \tag{10}$$

need to be chosen, leading to

$$B = \begin{cases} 1 & \text{for } \Lambda(B) > t \\ 1 & \text{for } \Lambda(B) = t \text{ with probability } (1-\omega) \\ 0 & \text{for } \Lambda(B) = t \text{ with probability } \omega \\ 0 & \text{for } \Lambda(B) < t \end{cases} \tag{11}$$

4. EXPERIMENTAL RESULTS

We consider the same experimental setup as in [2], i.e. the 3D scene depicted in Figure 5(a) consisting of several room items hidden behind a concrete wall. The scene is illuminated from two sides, using the synthetic aperture wideband TTW beamformer from [1]. The wall has a thickness of $5.625in$ and a dielectric constant $\epsilon = 7.66$. These parameters are assumed to be known when performing the beamforming. The synthetic aperture has a size of 57×57 elements with an interelement spacing of $0.875in$. The scene is illuminated using a stepped-frequency continuous-wave (CW) signal.

We consider the height of the metal dihedral, which is mounted on a high foam column, in the upper part of the room. Three B-Scans have been obtained with the following configurations:

- Image 1: Acquired from the front wall, using a stepped-frequency CW signal with bandwidth 800 MHz and a center frequency of 1.1 GHz.
- Image 2: Acquired from the front wall, using a stepped-frequency CW signal with bandwidth 800 MHz and a center frequency of 1.9 GHz.
- Image 3: Acquired from the side wall, using a stepped-frequency CW signal with bandwidth 2.4 GHz and a center frequency of 1.9 GHz.

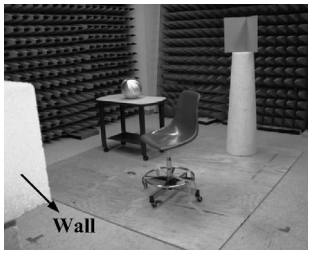

(a) 3D scene of interest

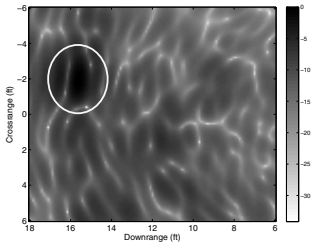

(b) Acquired B-scan 1

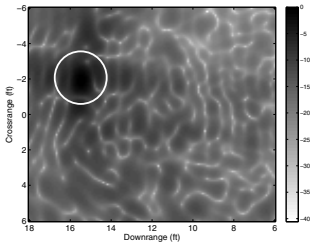

(c) Acquired B-scan 2

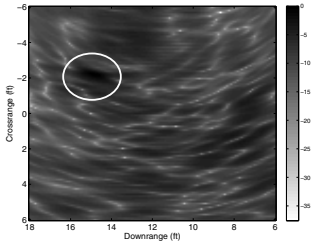

(d) Acquired B-scan 3

Fig. 5. Experimental setup

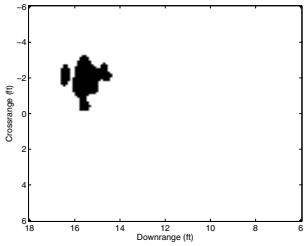

(a) Neyman-Pearson Test

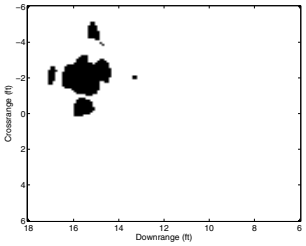

(b) Distributed Detector

Fig. 6. Experimental setup

The acquired images after background subtraction are shown in Figure 5(b-d), where the reflection due to the metal dihedral is marked in the upper left quarter. Given the distribution function under the null and alternative hypothesis for the images shown above, the probabilities of detection can be calculated via $P_D = \int_\gamma^\infty p(L|H_1)dL$. Due to the different statistics for all images, the following probabilities of detection are obtained for a fixed false-alarm rate $\alpha = 0.01\%$:

	Detector 1	Detector 2	Detector 3
Prob. of detection	0.898	0.916	0.73

The detection result when using the Neyman-Pearson test as in Equation (2) is shown in Figure 6(a). As can be seen, the metal dihedral is clearly detected. The clutter, which is visible in Figures 5(b-d) is strongly reduced by the image fusion. The distributed detection result using the optimal decision fusion derived in Equation (11) is shown in Figure 6(b). The metal dihedral is detected in the upper left quarter, but a slightly increased amount of clutter remains in the detected image. This stems from the fact that the Neyman-Pearson test uses the raw data set $\{Y_k(i,j)\}_{k=1}^K$, whereas in the case of distributed detection highly compressed information is transmitted to the fusion center, yielding a performance loss.

5. CONCLUSION

We introduced a framework for distributed detection and optimal decision fusion for Through-The-Wall Radar Imaging. The work has been focused on distributed Neyman-Pearson tests for dissimilar sensors. The optimum decision fusion scheme for three sensors has been presented and evaluated using experimental data. The use of a decentralized detection scheme has strong advantages in terms of the overall system reliability and reduction of computational cost. A small loss in performance has to be accepted compared to centralized detection schemes.

6. REFERENCES

[1] F. Ahmad and M. G. Amin, "Wideband synthetic aperture imaging for urban sensing applications," *Journal of the Franklin Institute*, vol. 345, no. 6, pp. 618–639, September 2008.

[2] C. Debes, M.G. Amin, and A.M. Zoubir, "Target detection in single- and multiple-view through-the-wall radar imaging," *IEEE Transactions on Geoscience and Remote Sensing*, vol. 47(5), pp. 1349 – 1361, 2009.

[3] C. Debes, J. Riedler, M. Amin, and A. Zoubir, "Iterative target detection approach for through-the-wall radar imaging," in *IEEE International Conference on Acoustics, Speech and Signal Processing (ICASSP)*, 2009, pp. 3061 – 3064.

[4] F. Ahmad, M.G. Amin, and G. Mandapati, "Autofocusing of through-the-wall radar imagery under unknown wall characteristics," *IEEE Transactions on Image Processing*, vol. 16, no. 7, pp. 1785–1795, July 2007.

[5] E.J. Baranoski, "Through wall imaging: Historical perspective and future directions," in *IEEE International Conference on Acoustics, Speech and Signal Processing*, 2008, pp. 5173–5176.

[6] S. M. Kay, *Fundamentals of Statistical Signal Processing, Volume 2: Detection Theory*, Prentice Hall PTR, 1998.

[7] R. Viswanathan and P.K. Varshney, "Distributed detection with multiple sensors I. Fundamentals," *Proceedings of the IEEE*, vol. 85, no. 1, pp. 54–63, 1997.

[8] R.S. Blum, S.A. Kassam, and H.V. Poor, "Distributed detection with multiple sensors II. Advanced topics," *Proceedings of the IEEE*, vol. 85, no. 1, pp. 64–79, 1997.

[9] S.C.A. Thomopoulos, R. Viswanathan, and D.C. Bougoulias, "Optimal decision fusion in multiple sensor systems," *IEEE Transactions on Aerospace and Electronic Systems*, vol. AES-23, no. 5, pp. 644–653, 1987.